



# Broadband light scattering of two relaxation processes in relaxor ferroelectric 0.93Pb(Zn<sub>1/3</sub>Nb<sub>2/3</sub>)O<sub>3</sub>-0.07PbTiO<sub>3</sub> single crystals

著者	Tsukada Shinya, Kojima Seiji
journal or publication title	Physical review B
volume	78
number	14
page range	144106
year	2008-10
権利	(C)2008 The American Physical Society
URL	<a href="http://hdl.handle.net/2241/101217">http://hdl.handle.net/2241/101217</a>

doi: 10.1103/PhysRevB.78.144106

# Broadband light scattering of two relaxation processes in relaxor ferroelectric $0.93\text{Pb}(\text{Zn}_{1/3}\text{Nb}_{2/3})\text{O}_3\text{-}0.07\text{PbTiO}_3$ single crystals

Shinya Tsukada<sup>1,2,\*</sup> and Seiji Kojima<sup>1,†</sup><sup>1</sup>*Graduate School of Pure and Applied Sciences, University of Tsukuba, Tsukuba, Ibaraki 305-8573, Japan*<sup>2</sup>*Japan Society for the Promotion of Science, Chiyoda, Tokyo 102-8471, Japan*

(Received 7 June 2008; revised manuscript received 27 August 2008; published 17 October 2008)

Dynamical properties of relaxor ferroelectric  $0.93\text{Pb}(\text{Zn}_{1/3}\text{Nb}_{2/3})\text{O}_3\text{-}0.07\text{PbTiO}_3$  single crystals have been studied by the broadband inelastic light scattering from gigahertz to terahertz frequency range. The longitudinal- and transverse-acoustic (LA and TA) phonon frequencies deviate below the Burns temperature  $T_B=736$  K from a linear temperature dependence above  $T_B$ , indicating the existence of polarization relaxations induced by the polar nanoregions (PNRs). On further cooling, a central peak (CP) which originates from the relaxations in the PNRs is observed clearly below  $600\text{ K} < T_B$ . The CP width decreases markedly down to  $T^*=499$  K and the change in the CP width becomes mild below  $T^*$ . The slower ( $\sim 10^{-12}$  s) and faster ( $\sim 10^{-13}$  s) relaxation times determined by the CP show good agreement with the relaxation times determined by TA and LA phonons, respectively.  $180^\circ$  and non- $180^\circ$  ( $71^\circ$  and  $109^\circ$ ) polarization flippings are allowed in the PNRs with the polar rhombohedral symmetry. Considering the piezoelectric coupling in a PNR, it is suggested that  $180^\circ$  flipping is related to the relaxation observed in LA phonon, while non- $180^\circ$  flipping is related to that in TA phonon.

DOI: [10.1103/PhysRevB.78.144106](https://doi.org/10.1103/PhysRevB.78.144106)

PACS number(s): 77.80.Bh, 78.35.+c, 77.84.Dy

## I. INTRODUCTION

One of the most attractive topics in condensed-matter physics is the relaxor ferroelectrics that are characterized by their nanoscopic structure, the so-called polar nanoregion (PNR).<sup>1,2</sup> The PNR arises from the chemical and valence mixing, which leads to the local polar structure in the nanometer scale. The PNRs in relaxor ferroelectrics generate the fluctuation in the macroscopic polarization, which causes the different ferroelectric-phase-transition behavior from normal ferroelectric ones. Understanding of such a nanoscopic structure and how the nanoscopic structure affects macroscopic phenomena such as ferroelectric phase transitions is a goal in many works.

Many kinds of measurements such as neutron scattering, dielectric constant, and far-infrared transmission spectroscopy have been performed to make the behavior clear.<sup>1-3</sup> Light-scattering measurement is one of them.<sup>4-7</sup> A central peak (CP) which is a peak at zero-frequency shift in a light-scattering spectrum can be used to investigate lattice relaxation from megahertz to terahertz of which polarizability varies with time. (In the inelastic-neutron-scattering spectrum, it is called “quasielastic scattering.”) Generally, the CP can originate from several phenomena related to the polarizability, e.g., phonon-density fluctuation, ion hopping, and flipping precursor cluster.<sup>8,9</sup> In the case of relaxor ferroelectrics, softening transverse-optical phonon inside PNRs exists above the Burns temperature  $T_B$ , then the CP appears.<sup>1,2</sup> Therefore, the induced local polarization inside the PNRs (precursor cluster) is the most probable origin of the relaxation unit observed in the CP.<sup>4-7</sup> As expected based on the polarization relaxation (change in dipole moments), the CP is also observed in infrared transmission spectroscopy (IR active) as well as neutron-inelastic-scattering measurements.<sup>10,11</sup> Since Jeong *et al.*<sup>12</sup> proposed that an order-disorder-type ordering of PNRs determines the long-

range polarizations, this study on the relaxation by observing the CP must be a key to the ferroelectric phase transition in relaxor ferroelectrics.

In view of the macroscopic properties, the PNRs are seen as polarization fluctuations in the electric properties such as dielectric susceptibility.<sup>1</sup> The acoustic properties are also affected by the behavior of the PNRs because the strain and the polarization couples: the acoustic waves modulate the magnitude of the ion displacements (magnitude of the local polarization). As a result of the behavior of the PNRs, the acoustic phonon shows extra softening and extra damping near a structural-phase-transition temperature.<sup>4,7</sup> The extra softening and damping can be interpreted by assuming a single relaxation of the local polarization inside the PNRs, which are based on the Landau-Khalatnikov equation of motion.<sup>7,13,14</sup> Consequently, two kinds of relaxation times (determined by the CP and acoustic phonon at gigahertz range) are obtained by measuring light scattering from gigahertz to terahertz range. Because both the relaxations observed in the CP and in the acoustic properties are attributed to the same origin (relaxation of local polarization in the PNRs), it is interesting to compare their time scales for more concrete discussion on the PNR.

The present paper reports on the temperature dependence of inelastic-light-scattering spectra of  $0.93\text{Pb}(\text{Zn}_{1/3}\text{Nb}_{2/3})\text{O}_3\text{-}0.07\text{PbTiO}_3$  (PZN-0.07PT) crystals. By analyzing the CP and the acoustic phonons (Brillouin scattering), the relaxation times are determined and they are compared with each other. In the  $(1-x)\text{Pb}(\text{Zn}_{1/3}\text{Nb}_{2/3})\text{O}_3\text{-}x\text{PbTiO}_3$  system, the composition  $x=0.07$  is close to the morphotropic phase boundary at  $x=0.09$ . The characteristic temperatures for the PNRs of PZN-0.07PT are already known: the PNRs appear below  $T_B=736$  K, and the growth of the PNRs starts to be suppressed below  $T^*=499$  K.<sup>15,16</sup> The crystal structure of PZN-0.07PT changes from cubic to tetragonal at  $T_{C-T}\sim 410$  K

and from tetragonal to rhombohedral at  $T_{T-R} \sim 390$  K upon cooling.<sup>17</sup> Large single crystals of homogeneous PZN-0.07PT can now be grown. The other piece of single crystal from the same ingot was used in a recent neutron-scattering measurement.<sup>18</sup>

## II. EXPERIMENTAL

Single crystals of PZN-0.07PT with slightly yellow color were grown by the high-temperature flux technique with PbO-based fluxes at Microfine Materials Technologies.<sup>19</sup> Each surface was perpendicular to  $[100]_c$  of the pseudocubic orientations. Light scattering was measured by a high-contrast 3+3-pass tandem Fabry-Pérot interferometer (JRS Scientific Instruments). A diode-pumped solid-state laser (Coherent) with a single-frequency operation at 532 nm at 100 mW was used. A 90° A-scattering geometry with polarizer [vertical to horizontal (VH)] was used for observing a transverse-acoustic (TA) phonon and a CP at a wave vector  $k \sim 2\sqrt{2}/\lambda n_i$ , while a 180°-scattering geometry without polarizer [vertical to open (VO)] was measured for observing a longitudinal-acoustic (LA) phonon at  $k \sim 4\pi/\lambda$ , where  $\lambda$  represents the wavelength of the laser (532 nm) and  $n_i$  represents the refractive index of the sample ( $\sim 2.6$  in PZN at 532 nm).<sup>20</sup> In each scattering geometry, the observed acoustic phonons propagate along the  $[100]_c$  direction in a cubic phase (above  $T_{C-T}$ ). Before starting each measurement, the sample was annealed for 1 h at 823 K ( $>T_B \sim 730$  K) to remove any memory effect of previous treatments. The measurements were performed upon cooling.

## III. RESULTS AND DISCUSSION

Figure 1 gives the light-scattering spectra of PZN-0.07PT measured at 473 and 773 K under three conditions. A LA phonon is seen at 180°-scattering geometry without polarizer, while a TA phonon is seen at 90° A-scattering geometry in VH spectra above  $T_{C-T}$ . By considering the elasto-optical coefficient and macroscopic cubic symmetry of PZN-0.07PT, it is apparent that two peaks of LA and TA phonons are related to the complex-elastic-stiffness constants  $c_{11}^*$  and  $c_{44}^*$ , respectively.<sup>21</sup> Besides acoustic phonons, the CP is observed in the broad frequency range. The CP develops with a decrease in temperature and its intensity becomes maximum around  $T_{C-T}$ .

To extract the frequency shift, width, and intensity of each peak in the light-scattering spectra, we use Voigt functions, where a width of a Gaussian component in the Voigt function is fixed as an instrumental function. The determined parameters of the acoustic phonons, Brillouin shift  $\nu$ , full width at half maximum (FWHM)  $\Gamma$ , and integrated intensity  $I$  are shown in Fig. 2 as functions of temperature. The anomalous behavior of the acoustic phonons is seen around  $T_{C-T}$  in a wide temperature range. The softening of LA and TA phonons is due to the condensation of dynamic PNRs (ergodic state) into static PNRs (nonergodic state) or macroscopic ferroelectric domains. The developed fluctuation (imaginary part of the complex elastic constant which is proportional to  $\Gamma_B$ ) results from energy dissipation and the en-

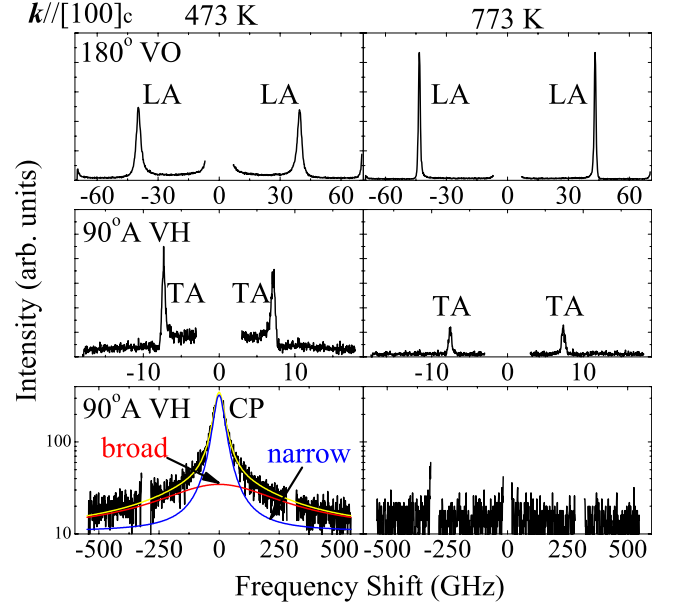


FIG. 1. (Color online) Light-scattering spectra at 473 and 773 K in different conditions. Peaks at non-zero-frequency shift denote the Brillouin scattering, which are attributed to LA and TA phonons. CP denotes a central peak observed at zero-frequency shift. Only broadband spectra are shown in semilogarithmic plot. Fit result of a CP is shown (left bottom). Note that 1 [meV] = 242 [GHz].

ergy transfers to other degrees of freedom.<sup>22</sup>  $I$  is proportional to the susceptibility of the lattice vibration.  $\chi(0)$  as  $I = k_B T \chi(0)$ , where  $k_B$  denotes the Boltzmann constant, and its maximum at  $T_{C-T}$  indicates that the acoustic phonon becomes unstable because of the structural transformation. Compared with normal ferroelectrics, the temperature range of the anomaly is much broader because the fluctuation in

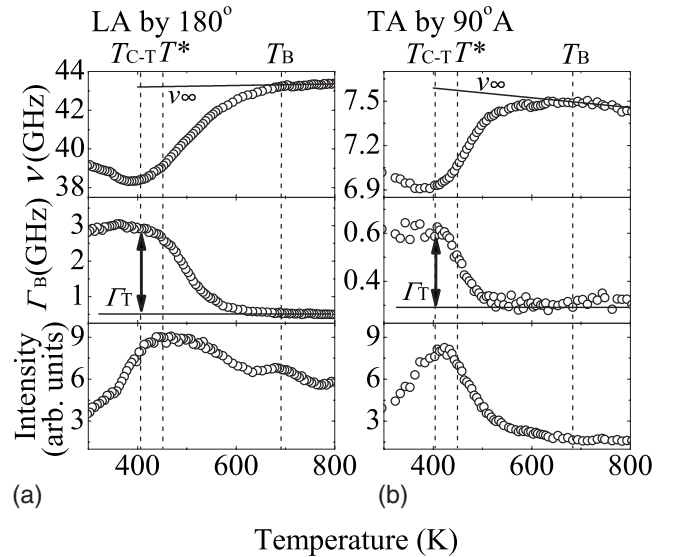


FIG. 2. Temperature dependences of Brillouin shift, FWHM, and integrated intensity on cooling at (a) 180°-scattering geometry and (b) 90° A-scattering geometry. Solid lines are curves fitted with  $\nu_\infty = A - BT$  above  $T_B$ , where  $A$  and  $B$  are constants.  $\Gamma_T$  denotes the FWHM related to the phase transition.

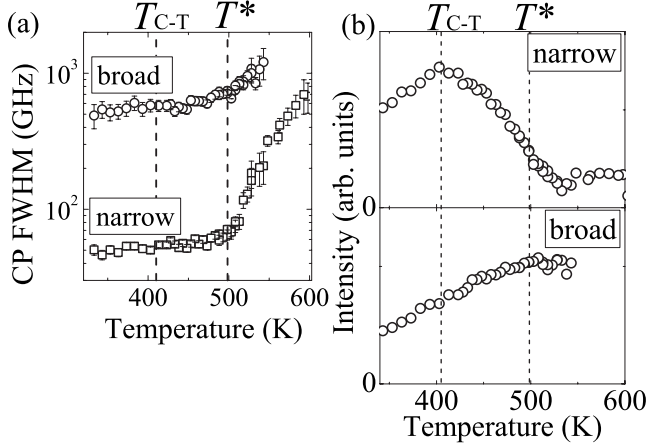


FIG. 3. Temperature dependences of (a) FWHM and (b) intensity of each Voigt function which are used for fitting the CP (Fig. 1), where the width of the Gaussian function is fixed with that of an instrumental broadening.

polarization is induced by the PNRs below  $T_B$  in a wide temperature range.<sup>20</sup> As a result, the critical region in PZN-0.07PT appears in the wide temperature range. In addition, around  $T_{C-T}$ , both frequencies of LA and TA phonons show minima; i.e., the fluctuations do not diverge. This is related with the fact that the PNRs persist even in the low-temperature phase.<sup>1,2</sup> Short-range order can exist with long-range ferroelectric order, which is also a characteristic property of relaxor ferroelectric materials.

The fit parameters of the CP (FWHM  $\Gamma_{CP}$  and intensity) are shown in Fig. 3. The CP cannot be reproduced by assuming single-relaxation process, which is consistent with the previous works on  $0.71\text{Pb}(\text{Ni}_{1/3}\text{Nb}_{2/3})\text{O}_3\text{-}0.29\text{PbTiO}_3$  (PNN-0.29PT).<sup>6,7</sup> So in this study, the CP was fitted by two Voigt functions, which assumes that the CP originates from two single-relaxation processes. Figure 3 shows that  $\Gamma_{CP}$  narrows on cooling from high temperature to  $T^*$ . It must be related to the behavior of the PNRs, which is described in the latter part.

To determine the characteristic time of the polarization fluctuation  $\tau_B$  by the acoustic phonons, we used Eq. (1) assuming that single relaxation occurs at each phonon-frequency range,<sup>7,23</sup>

$$\tau_B = \frac{\Gamma_T}{2\pi(\nu_\infty^2 - \nu^2)}, \quad (1)$$

where  $\nu_\infty$  denotes the Brillouin shift at a high-frequency limit.  $\Gamma_T$  is the FWHM related to the phase transition as shown in Fig. 2. At a sufficiently high-temperature range ( $>T_B$ ), relaxor ferroelectrics are in the paraelectric phase without any PNRs. In this temperature range,  $\nu$  shows the linear temperature dependence, which is only due to the lattice anharmonicity.<sup>7</sup> We used the linearly temperature-dependent  $\nu$  at high temperature as  $\nu_\infty$  as shown in Fig. 2. This is reasonable because the electrostrictive coupling is the main coupling term in the free-energy expansion in the cubic phase of relaxor ferroelectrics.<sup>4,7,13,23</sup> Two relaxation times determined by LA phonon in  $180^\circ$ -scattering geometry ( $\tau_{LA}^{180}$ )

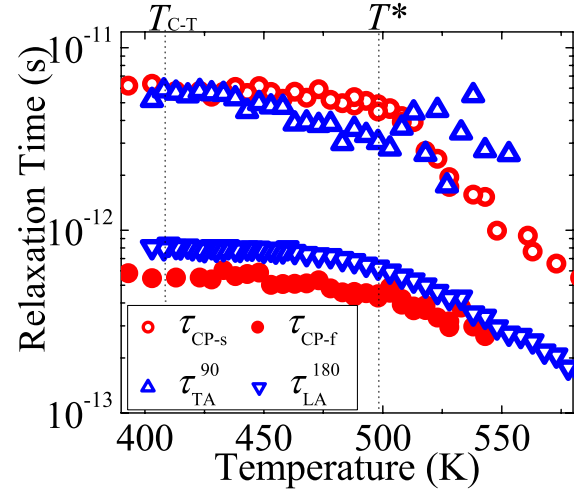


FIG. 4. (Color online) Temperature dependences of the relaxation times of the polarization inside PNRs determined by Eqs. (1) and (2).

and TA phonon in  $90^\circ$  A-scattering geometry ( $\tau_{TA}^{90}$ ) are shown in Fig. 4 as functions of temperature. Their time scales are between  $10^{-11}$  and  $10^{-13}$  s.  $\tau_{LA}$  is interpreted as a fluctuation accompanied by a volume change at a phonon frequency, while  $\tau_{TA}$  is interpreted as a fluctuation without a volume change at a phonon frequency.<sup>7,24</sup>

The relaxation time was determined by CP assuming the Debye-relaxation process as

$$\pi\Gamma_{CP}\tau_{CP} = 1, \quad (2)$$

and two relaxation times  $\tau_{CP}$  are determined by substituting FWHM of CP for  $\Gamma_{CP}$  in Fig. 4(a). We denote the faster relaxation time as  $\tau_{CP-f}$  and the slower relaxation time as  $\tau_{CP-s}$ . Their temperature dependences are illustrated in Fig. 4 together with  $\tau_{TA}^{90}$  and  $\tau_{LA}^{180}$ . From Fig. 4, we can say that  $\tau_{CP-f}$  is compatible with  $\tau_{LA}^{180}$ , while  $\tau_{CP-s}$  is compatible with  $\tau_{TA}^{90}$ . The agreement of  $\tau_{CP-f}$  with  $\tau_{LA}^{180}$  is also seen in PNN-0.29PT.<sup>9</sup> As mentioned in Sec. I, the relaxation unit is the local polarization inside the PNRs, and its relaxation means that the local polarization flips from one direction to the other. The PNR has rhombohedral symmetry with the polar axis along the  $[111]_c$  direction ( $[001]$  for trigonal coordinate), which is determined by means of dynamical structural analysis of diffuse neutron scattering and dynamic pair-distribution function (PDF) of pulsed neutron inelastic scattering in  $\text{Pb}(\text{Mg}_{1/3}\text{Nb}_{2/3})\text{O}_3$  (PMN) and PZN-xPT (Refs. 12 and 25–27); i.e., the local polarization direction in the PNRs fluctuates in the eight equivalent  $[111]_c$  directions. There are three kinds of polarization reorientation processes in PNRs,  $180^\circ$ ,  $71^\circ$ , and  $109^\circ$  flippings.<sup>28</sup> The schematic diagram of each flipping is shown in Fig. 5. The  $180^\circ$  flipping occurs without the change in local shear strain in the PNRs and its switching rate is fast. On the other hand, non- $180^\circ$  ( $71^\circ$  and  $109^\circ$ ) flipping occurs with the change in the local shear strain and its switching rate is slow because the motion accompanying strain can be slower than that without accompanying strain.<sup>28</sup> This fact indicates that the faster relaxation process ( $\tau_{CP-f}$  and  $\tau_{LA}^{180}$ ) is attributed to the  $180^\circ$  dipole flip-

ping and the other ( $\tau_{\text{CP-S}}$  and  $\tau_{\text{TA}}^{\text{90}}$ ) is attributed to the non-180° dipole flipping.<sup>6</sup>

To make clear the above discussion, we approach it from the view of symmetry treatment. When the 180° flipping occurs, only the diagonal sections of the strain tensor  $s_{ij}$  ( $i$  and  $j=1, 2$ , and 3) change through the piezoelectric coupling in the PNRs as Eq. (3) because the structure inside the PNR is polar rhombohedral and piezoelectric coupling is the main coupling term between the local polarization inside PNR and the strain;<sup>25-27</sup>

$$\begin{pmatrix} s_{11} & s_{12} & s_{13} \\ s_{12} & s_{22} & s_{23} \\ s_{13} & s_{23} & s_{33} \end{pmatrix} = \begin{pmatrix} 0 & 0 & P_3 \end{pmatrix} \times \begin{pmatrix} 0 & 0 & 0 & 0 & d_{15} & 2d_{21} \\ d_{21} & -d_{21} & 0 & d_{15} & 0 & 0 \\ d_{31} & d_{31} & d_{33} & 0 & 0 & 0 \end{pmatrix} = \begin{pmatrix} P_3 d_{31} & 0 & 0 \\ 0 & P_3 d_{31} & 0 \\ 0 & 0 & P_3 d_{33} \end{pmatrix} \quad (3)$$

to

$$\begin{pmatrix} s_{11} & s_{12} & s_{13} \\ s_{12} & s_{22} & s_{23} \\ s_{13} & s_{23} & s_{33} \end{pmatrix} = A^{-1} \begin{pmatrix} P_3 d_{31} & 0 & 0 \\ 0 & P_3 d_{31} & 0 \\ 0 & 0 & P_3 d_{33} \end{pmatrix} A = \begin{pmatrix} P_3 d_{31} & 0 & 0 \\ 0 & (P_3 d_{31} + 8P_3 d_{33})/9 & 2\sqrt{2}(P_3 d_{33} - P_3 d_{31})/9 \\ 0 & 2\sqrt{2}(P_3 d_{33} - P_3 d_{31})/9 & (8P_3 d_{31} + P_3 d_{33})/9 \end{pmatrix}, \quad (5)$$

where  $A$  in the above expression denotes the representation matrix used to convert basis vectors from before to after 71° flipping as shown in Fig. 5,

$$A = \begin{pmatrix} -1 & 0 & 0 \\ 0 & -1/3 & 2\sqrt{2}/3 \\ 0 & 2\sqrt{2}/3 & 1/3 \end{pmatrix}. \quad (6)$$

The change in  $s_{ij}$  from Eq. (3) to Eq. (5) indicates that the change in the strain by 71° flipping is related to both LA and TA phonons. However, the sum of the diagonal sections related to LA phonon does not change. On the other hand, that of off-diagonal sections changes markedly. As a result, the change in the strain by 71° flipping is mainly related with TA phonon. The change in the strain by 109° flipping is also derived easily and it is also mainly related to TA phonon. Consequently, the origin of the narrow component of the CP is non-180° (71° and 109°) flipping. Note that we observe the light scattering at small  $k$  (at long-wavelength range which is larger than the size of the PNRs). Therefore, we mean that the narrow CP and the broad CP originate from the collective character of the flipping (reorientation) of the PNRs, and we suggest the microscopic motion in a PNR as

$$\begin{pmatrix} s_{11} & s_{12} & s_{13} \\ s_{12} & s_{22} & s_{23} \\ s_{13} & s_{23} & s_{33} \end{pmatrix} = \begin{pmatrix} 0 & 0 & -P_3 \end{pmatrix} \times \begin{pmatrix} 0 & 0 & 0 & 0 & d_{15} & 2d_{21} \\ d_{21} & -d_{21} & 0 & d_{15} & 0 & 0 \\ d_{31} & d_{31} & d_{33} & 0 & 0 & 0 \end{pmatrix} = \begin{pmatrix} -P_3 d_{31} & 0 & 0 \\ 0 & -P_3 d_{31} & 0 \\ 0 & 0 & -P_3 d_{33} \end{pmatrix}, \quad (4)$$

where  $P_3$  and  $d_{ij}$  denote the polarization along  $[111]_c$  and the piezoelectric constants in the trigonal coordinate, respectively. It indicates that the change in the strain by 180° flipping is only related with LA phonon. In other words, the origin of the broad component of the CP is 180° flipping.

In the case of 71° flipping, the strain tensor changes from Eq. (3) to

shown in Fig. 5. Even in the case where the structure of the PNRs is tetragonal or orthorhombic with the spontaneous polarization along the main axis,<sup>29</sup> our interpretation using the strain matrix can be applied and it is similarly concluded: 180° and non-180° (90°) local polarization flippings cause the softening of LA and TA phonons, respectively.

In some Pb-free perovskite structure, e.g.,  $\text{KTa}_{1-x}\text{Nb}_x\text{O}_3$ , 180° flipping is not usual, and it is considered that non-180° flipping dominates the CP behavior.<sup>30</sup> This is because the hopping of the  $B$ -site ion in the perovskite structure is the origin of the local polarization in the case of normal perovskite ferroelectrics. On the other hand, in Pb-containing relaxor ferroelectrics, every ion shows displacement from their ideal positions of the cubic perovskite structure.<sup>1,12,26,27</sup> These displacements make the properties of relaxor ferroelectrics more complicated. Current studies on the pressure dependence of atomic displacements in PMN and  $\text{Pb}(\text{Mg}_{1/3}\text{Ta}_{2/3})\text{O}_3$  demonstrate that only Pb ion is sensitive to the pressure.<sup>31,32</sup> This implies that the local polarization in a PNR is mainly composed of Pb-ion displacement. Moreover, it was reported that Pb ions have correlated with not only the  $[111]_c$  but also the  $[1\bar{1}0]_c$  direction.<sup>29,33</sup> As a result of such situation, 180° flipping can be seen apparently in the



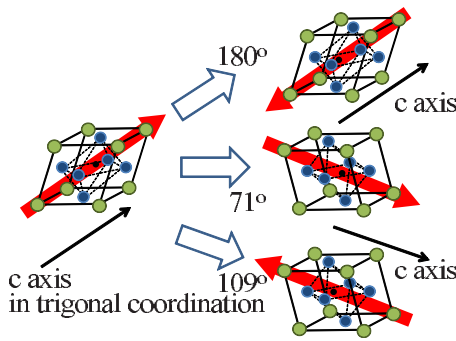


FIG. 5. (Color online) Schematic diagram of the polarization-relaxation processes in the PNRs.

relaxor ferroelectrics.

According to our results and previous works on PNN-0.29PT, the dynamical behavior of PNRs could be summarized as follows.<sup>6,7</sup> The PNRs appear below  $T_B$  because of the local Pb off-centering and local rhombohedral distortion induced by soft phonons.<sup>12,27,28</sup> The PNRs are dynamic and are not correlated with each other between  $T_B$  and  $T^*$  where the PNRs can grow on cooling. As a result of growing size, the relaxation behavior slows on cooling. Then, below  $T^*$ , all PNRs are correlated, which interrupts the growth of the PNRs. Therefore, the relaxation times are saturated below  $T^*$ . Finally, the PNRs interact with each other and induce structural phase transitions at  $T_{C-T}$  and  $T_{T-R}$ .

#### IV. CONCLUSIONS

In conclusion, relaxation processes in the PNRs have been studied in relaxor ferroelectric PZN-0.07PT single crystals by inelastic light scattering. A CP is measured in a broad frequency range from gigahertz to terahertz. The CP width shows narrowing markedly down to  $T^*=499$  K, which is related to the behavior of the PNRs. Anomalies in LA and TA phonons are observed below  $T_B$  because of the relaxations, and two relaxation times are determined by LA and TA phonons. The slower ( $\sim 10^{-12}$  s) and faster ( $10^{-13}$  s) relaxation times determined by the CP show good agreement with those by TA and LA phonons, respectively.  $180^\circ$  and non- $180^\circ$  ( $71^\circ$  and  $109^\circ$ ) local polarization flippings are allowed in the PNRs with the polar rhombohedral symmetry. Based on the change in the local strain in the PNRs, we consider that the faster relaxation originates from  $180^\circ$  flipping, while the slower relaxation originates from non- $180^\circ$  flipping, of which freezing processes determine the long-range polarization behaviors below  $T_{C-T}$ .

#### ACKNOWLEDGMENTS

The authors thank I.-K. Jeong, K. Ohwada, Y. Yoneda, M. Iwata, and S.-I. Ikeda for fruitful discussions and ideas. They give special thanks to J.-H. Ko for valuable discussions. They also thank S. Saito and M. Muroi for their technical support. This research was partially supported by the Research Foundation of the Japan Society for the Promotion of Science for Young Scientists (Grant No. 19-1404).

\*Corresponding author. FAX: +81-29-853-5262; s-tsukada@ims.tsukuba.ac.jp

†kojima@ims.tsukuba.ac.jp

<sup>1</sup>A. A. Bokov and Z.-G. Ye, J. Mater. Sci. **41**, 31 (2006).

<sup>2</sup>K. Hirota, S. Wakimoto, and D. E. Cox, J. Phys. Soc. Jpn. **75**, 111006 (2006).

<sup>3</sup>J. Hlinka, J. Petzelt, S. Kamba, D. Noujni, and T. Ostapchuk, Phase Transitions **79**, 41 (2006).

<sup>4</sup>J.-H. Ko, D. H. Kim, and S. Kojima, Phys. Rev. B **77**, 104110 (2008).

<sup>5</sup>O. Svitelskiy, J. Toulouse, G. Yong, and Z.-G. Ye, Phys. Rev. B **68**, 104107 (2003).

<sup>6</sup>S. Tsukada, Y. Ike, J. Kano, T. Sekiya, Y. Shimojo, R. Wang, and S. Kojima, Appl. Phys. Lett. **89**, 212903 (2006).

<sup>7</sup>S. Tsukada, Y. Ike, J. Kano, T. Sekiya, Y. Shimojo, R. Wang, and S. Kojima, J. Phys. Soc. Jpn. **77**, 033707 (2008).

<sup>8</sup>A. D. Bruce and R. A. Cowley, *Structural Phase Transitions* (Taylor & Francis, Oxford, 1981).

<sup>9</sup>P. A. Fleury and K. B. Lyons, in *Modern Problems in Condensed Matter Physics*, edited by V. M. Agranovich and A. A. Maradudin (North-Holland, Amsterdam, 1983), Vol. 5, Chap. 7, pp. 449–502.

<sup>10</sup>S. Kamba, M. Kempa, V. Bovtun, J. Petzelt, K. Brinkman, and N. Setter, J. Phys.: Condens. Matter **17**, 3965 (2005).

<sup>11</sup>H. Hiraka, S.-H. Lee, P. M. Gehring, G. Xu, and G. Shirane, Phys. Rev. B **70**, 184105 (2004).

<sup>12</sup>I.-K. Jeong, J. K. Lee, and R. H. Heffner, Appl. Phys. Lett. **92**, 172911 (2008).

<sup>13</sup>T. Yagi, M. Tokunaga, and I. Tatsuzaki, J. Phys. Soc. Jpn. **40**, 1659 (1976).

<sup>14</sup>W. Rehwald, Adv. Phys. **22**, 721 (1973).

<sup>15</sup>M. Roth, E. Mojaev, E. Dul'kin, P. Gemeiner, and B. Dkhil, Phys. Rev. Lett. **98**, 265701 (2007).

<sup>16</sup>E. Dul'kin, M. Roth, P.-E. Janolin, and B. Dkhil, Phys. Rev. B **73**, 012102 (2006).

<sup>17</sup>J. Kuwata, K. Uchino, and S. Nomura, Ferroelectrics **37**, 579 (1981).

<sup>18</sup>G.-M. Rotaru, S. N. Gvasaliya, B. Roessli, S. Kojima, S. G. Lushnikov, and P. Günter, Appl. Phys. Lett. **93**, 032903 (2008).

<sup>19</sup>L. C. Lim, K. K. Rajan, and J. Jin, IEEE Trans. Ultrason. Ferroelectr. Freq. Control **54**, 2474 (2007).

<sup>20</sup>G. Burns and F. H. Dacol, Solid State Commun. **48**, 853 (1983).

<sup>21</sup>W. Hayes and R. Loudon, *Scattering of Light by Crystals* (Dover, New York, 1978).

<sup>22</sup>L. D. Landau and E. M. Lifshitz, *Statistical Physics* (Butterworth-Heinemann, Oxford, 1980).

<sup>23</sup>Y. Tsujimi, T. Yagi, H. Yamashita, and I. Tatsuzaki, J. Phys. Soc. Jpn. **50**, 184 (1981).

<sup>24</sup>L. D. Landau and E. M. Lifshitz, *Theory of Elasticity* (Butterworth-Heinemann, Oxford, 1986).

<sup>25</sup>S. B. Vakhrushev, A. A. Naberezhnov, N. M. Okuneva, and B. N. Savenko, Phys. Solid State **37**, 1993 (1995).

- <sup>26</sup>W. Dmowski, S. B. Vakhrushev, I.-K. Jeong, M. P. Hehlen, F. Trouw, and T. Egami, *Phys. Rev. Lett.* **100**, 137602 (2008).
- <sup>27</sup>I.-K. Jeong and J. K. Lee, *Appl. Phys. Lett.* **88**, 262905 (2006).
- <sup>28</sup>S. Wada and T. Tsurumi, *Ferroelectrics* **261**, 305 (2001).
- <sup>29</sup>M. Paściak, M. Wołczyr, and A. Pietraszko, *Phys. Rev. B* **76**, 014117 (2007).
- <sup>30</sup>L. A. Knauss, X. M. Wang, and J. Toulouse, *Phys. Rev. B* **52**, 13261 (1995).
- <sup>31</sup>G.-M. Rotaru, S. N. Gvasaliya, V. Pomjakushin, B. Roessli, Th. Strassle, S. G. Lushnikov, T. A. Shaplygina, and P. Gunter, *J. Phys.: Condens. Matter* **20**, 104235 (2008).
- <sup>32</sup>S. N. Gvasaliya, V. Pomjakushin, B. Roessli, Th. Strässle, S. Klotz, and S. G. Lushnikov, *Phys. Rev. B* **73**, 212102 (2006).
- <sup>33</sup>D. La-Orautapong, J. Toulouse, Z.-G. Ye, W. Chen, R. Erwin, and J. L. Roberston, *Phys. Rev. B* **67**, 134110 (2003).